View metadata, citation and similar papers at core.ac.uk

brought to you by CORE

provided by Elsevier - Publisher Connector

Modulation of D2R-NR2B Interactions in Response to Cocaine

Xian-Yu Liu,[1] Xiang-Ping Chu,[3] Li-Min Mao,[1]
Min Wang,[4] Hong-Xiang Lan,[5] Ming-Hua Li,[3]
Guo-Chi Zhang,[1] Nikhil K. Parelkar,[1]
Eugene E. Fibuch,[2] Michelle Haines,[2] Kim A. Neve,[5]
Fang Liu,[4] Zhi-Gang Xiong,[3] and John Q. Wang[1,2,*]

[1] Department of Basic Medical Science
[2] Department of Anesthesiology
University of Missouri-Kansas City
School of Medicine
Kansas City, Missouri 64108

[3] Robert S. Dow Neurobiology Laboratories
Legacy Research
Portland, Oregon 97232

[4] Department of Neuroscience
Centre for Addiction and Mental Health
University of Toronto
Toronto, Ontario, M5T 1R8
Canada

[5] Department of Behavioral Neuroscience
Oregon Health and Science University
and Veterans Affairs Medical Center
Portland, Oregon 97239

Summary

Dopamine-glutamate interactions in the neostriatum determine psychostimulant action, but the underlying molecular mechanisms remain elusive. Here we found that dopamine stimulation by cocaine enhances a heteroreceptor complex formation between dopamine D2 receptors (D2R) and NMDA receptor NR2B subunits in the neostriatum in vivo. The D2R-NR2B interaction is direct and occurs in the confined postsynaptic density microdomain of excitatory synapses. The enhanced D2R-NR2B interaction disrupts the association of Ca^{2+}/calmodulin-dependent protein kinase II (CaMKII) with NR2B, reduces NR2B phosphorylation at a CaMKII-sensitive site (Ser1303), and inhibits NMDA receptor-mediated currents in medium-sized striatal neurons. Furthermore, the regulated D2R-NR2B interaction is critical for constructing behavioral responsiveness to cocaine. Our findings here uncover a direct and dynamic D2R-NR2B interaction in striatal neurons in vivo. This type of dopamine-glutamate integration at the receptor level may be responsible for synergistically inhibiting the D2R-mediated circuits in the basal ganglia and fulfilling the stimulative effect of psychostimulants.

Introduction

Ionotropic glutamate receptors play a significant role in the regulation of a variety of cellular and synaptic activities, including learning and memory (Zorumski and Izumi, 1998), the effectiveness of addictive and neurotoxic properties of drugs of abuse (Wolf, 1998; Kalivas, 2004; Nestler, 2005), and phenotypes of various forms of neurodegenerative diseases (Sattler and Tymianski, 2001). The major members of ionotropic glutamate receptors include NMDA receptor (NMDAR) and non-NMDAR (AMPA and kainate) subclasses. Each subclass of receptors is a heteromultimer of core subunits that form a functional ion channel. NMDARs are assembled with the obligatory NR1 subunit and one or more modulatory NR2A–D subunits. Various subunit compositions determine the channel property and function.

Protein phosphorylation is an important mechanism for the posttranslational modulation of glutamate receptor function (Wang et al., 1993; Wang and Salter, 1994; Lau and Huganir, 1995; Rostas et al., 1996). Similar to NR1 (Tingley et al., 1997), NR2B is phosphorylated at C-terminal Ser1303 (Omkumar et al., 1996) and several tyrosine sites (Wang and Salter, 1994; Nakazawa et al., 2001). The Ser1303 phosphorylation is driven by Ca^{2+}/calmodulin-dependent protein kinase II (CaMKII), an abundant kinase in the postsynaptic density (PSD) of glutamatergic synapses (Kelly et al., 1984), or protein kinase C (PKC) (Liao et al., 2001). Available evidence consistently shows that the NR2B phosphorylation at either serine or tyrosine sites positively regulates NMDAR-mediated currents (Lieberman and Mody, 1994; Wang and Salter, 1994; Liao et al., 2001; Rostas et al., 1996) and affects NMDAR signaling via regulating receptor trafficking and interactions with synaptic scaffold/signaling proteins (Hall and Soderling, 1997; Dunah et al., 2004; Chung et al., 2004).

The neostriatum is a major structure in the basal ganglia regulating extrapyramidal motor and cognitive behaviors. This structure has also been the focus of experimental studies aimed to illustrate brain mechanisms for psychostimulant actions (Hyman and Malenka, 2001; Nestler, 2005). Activation of dopaminergic transmission in this region has been well documented to mediate effects of dopamine stimulants (Koob and Nestler, 1997; Berke and Hyman, 2000; Vanderschuren and Kalivas, 2000). Similarly, glutamatergic transmission plays an active role in drug actions (Wolf, 1998; Wang and McGinty, 1999; Kalivas, 2004) as the striatum is abundantly innervated with glutamatergic afferents, and NMDARs, principally NR1 and NR2B subunits, are densely expressed in striatal neurons (Standaert et al., 1999; Landwehrmeyer et al., 1995; Chen and Reiner, 1996; Kuppenbender et al., 2000). It is known that the two transmitter systems intimately interact with each other to mediate drug actions, but the molecular mechanisms underlying their interactions are poorly understood.

We therefore investigated dopamine-glutamate interactions by examining phosphorylation of a prevalent NMDAR subunit (NR2B) in the striatum after dopamine stimulation in vivo. We found that acute cocaine specifically reduced Ser1303 phosphorylation via a dopamine D2 receptor (D2R)-mediated mechanism. Interestingly, D2Rs directly interacted with NR2B and disrupted the NR2B-CaMKII binding, leading to inhibition of Ser1303 phosphorylation. Furthermore, the D2R-NR2B interaction was critical for modulating NMDAR-mediated currents and behavioral responsiveness to cocaine.

*Correspondence: wangjq@umkc.edu

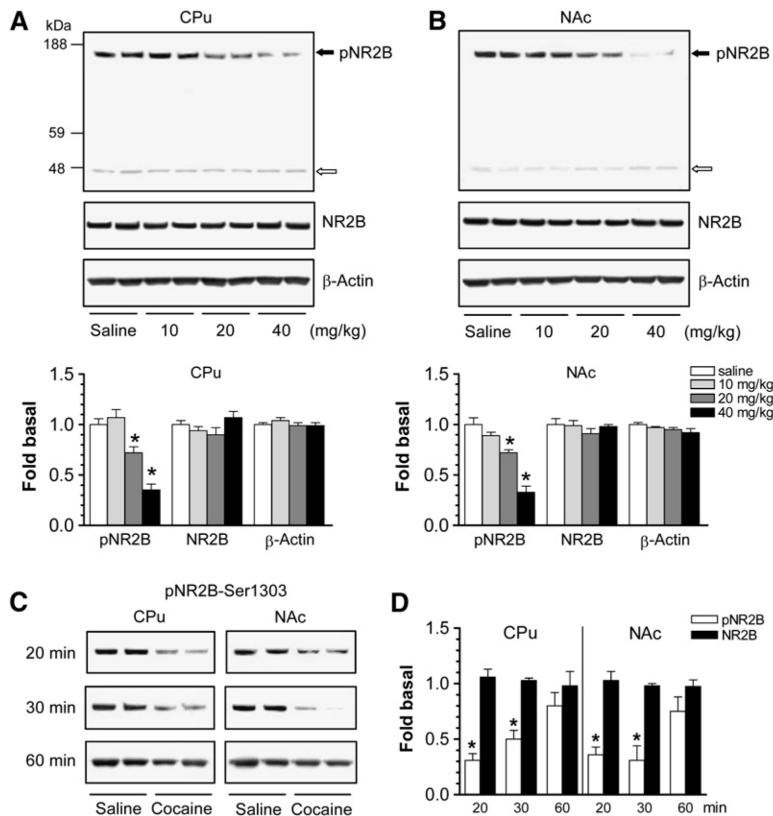

Figure 1. Cocaine Reduces NR2B Phosphorylation at Ser1303 in the Rat Striatum

(A and B) Cocaine dose-dependently reduced basal levels of pNR2B-Ser1303, but not NR2B and β-actin, in the CPu and NAc. Cocaine was injected at three different doses (10, 20, or 40 mg/kg, i.p.) and rats were sacrificed 30 min after saline or cocaine injection. Representative immunoblots are shown above the quantified data. The solid arrows indicate pNR2B-Ser1303 bands whereas open arrows indicate weak cross-reactive bands detected by the anti-pNR2B-Ser1303 antibody.

(C and D) Cocaine time-dependently reduced basal levels of pNR2B-Ser1303, but not NR2B, in the CPu and NAc. Cocaine was injected at 30–40 mg/kg (i.p.) and rats were sacrificed at indicated time points after saline or cocaine injection. Data are presented as means ± SEM from five to six experiments. *$p < 0.05$ versus saline.

Results

Reduction of NR2B Phosphorylation: Generality, Specificity, and Spatiotemporal Characteristics

To examine the effect of cocaine on NR2B phosphorylation, we measured changes in phosphorylation of NR2B at Ser1303 and Tyr1336 in the striatum following acute cocaine stimulation in vivo. Phospho-site-specific antibodies were used to detect these changes (see Figure S1 in the Supplemental Data for a validation of the selectivity of these antibodies). A single intraperitoneal (i.p.) injection of cocaine (10, 20, or 40 mg/kg) dose-dependently reduced pNR2B-Ser1303 levels in both the dorsal (caudate putamen, CPu) and ventral (nucleus accumbens, NAc) striatum (Figures 1A and 1B). Cocaine at all doses showed no effect on total levels of NR2B or β-actin. Thus, the reduction of the phospho-NR2B proteins resulted from decreased phosphorylation rather than a reduced amount of NR2B. Cocaine at all doses did not significantly alter pNR2B-Tyr1336 levels in the dorsal and ventral striatum (data not shown) in contrast to the profound decrease in pNR2B-Ser1303 levels. Thus, cocaine selectively decreases NR2B phosphorylation at a serine site. To disclose the kinetic property of the cocaine effect, we performed a time course study in which cocaine at 30–40 mg/kg was injected and rats were sacrificed at three different time points after drug injection. We found that cocaine induced a rapid and reversible reduction of Ser1303 phosphorylation (Figures 1C and 1D). At all time points surveyed, cocaine showed no effect on total NR2B and β-actin expression.

In the above dose-response and time course studies, the reduction of Ser1303 phosphorylation was not confined to the CPu nor the NAc of the striatum. In addition to the striatum, other forebrain and midbrain areas were tested for changes in Ser1303 phosphorylation. Cocaine (10, 20, or 40 mg/kg, i.p., 30 min) did not alter pNR2B-Ser1303 and NR2B levels in the frontal cortex, the hippocampus, the ventral tegmental area, or the amygdala (Figure S2). Thus, cocaine induced a region-specific inhibition of NR2B phosphorylation in the striatum.

The Role of Dopamine Receptors in Regulating NR2B Phosphorylation

Cocaine is known to stimulate dopamine receptors through enhanced synaptic dopamine availability in the striatum by blocking the reuptake of released dopamine into the presynaptic terminal (Hurd and Ungerstedt, 1989; Kalivas and Duffy, 1993). There are two major classes of dopamine receptors: a D1 class (D1 and D5 subtypes) and a D2 class (D2, D3, and D4 subtypes), with the D1 and D2 subtypes being the most highly enriched in the mammalian striatum (Gerfen, 2000). To evaluate the role of D1Rs and D2Rs in mediating the cocaine effect, we measured effects of a D1R or D2R selective antagonist on the cocaine inhibition of Ser1303 phosphorylation. In a first attempt to examine roles of D1Rs and D2Rs in regulating constitutive NR2B phosphorylation, we found that neither the D1R antagonist SCH23390 (0.1 mg/kg) nor the D2R antagonist eticlopride (0.5 mg/kg) altered basal levels of pNR2B-Ser1303 in the CPu and NAc (Figure 2A). Thus, under normal conditions, endogenous dopaminergic tone on D1Rs or D2Rs has a minimal influence over NR2B phosphorylation. Furthermore, SCH23390 had no effect on the cocaine-induced reduction of pNR2B-Ser1303 levels

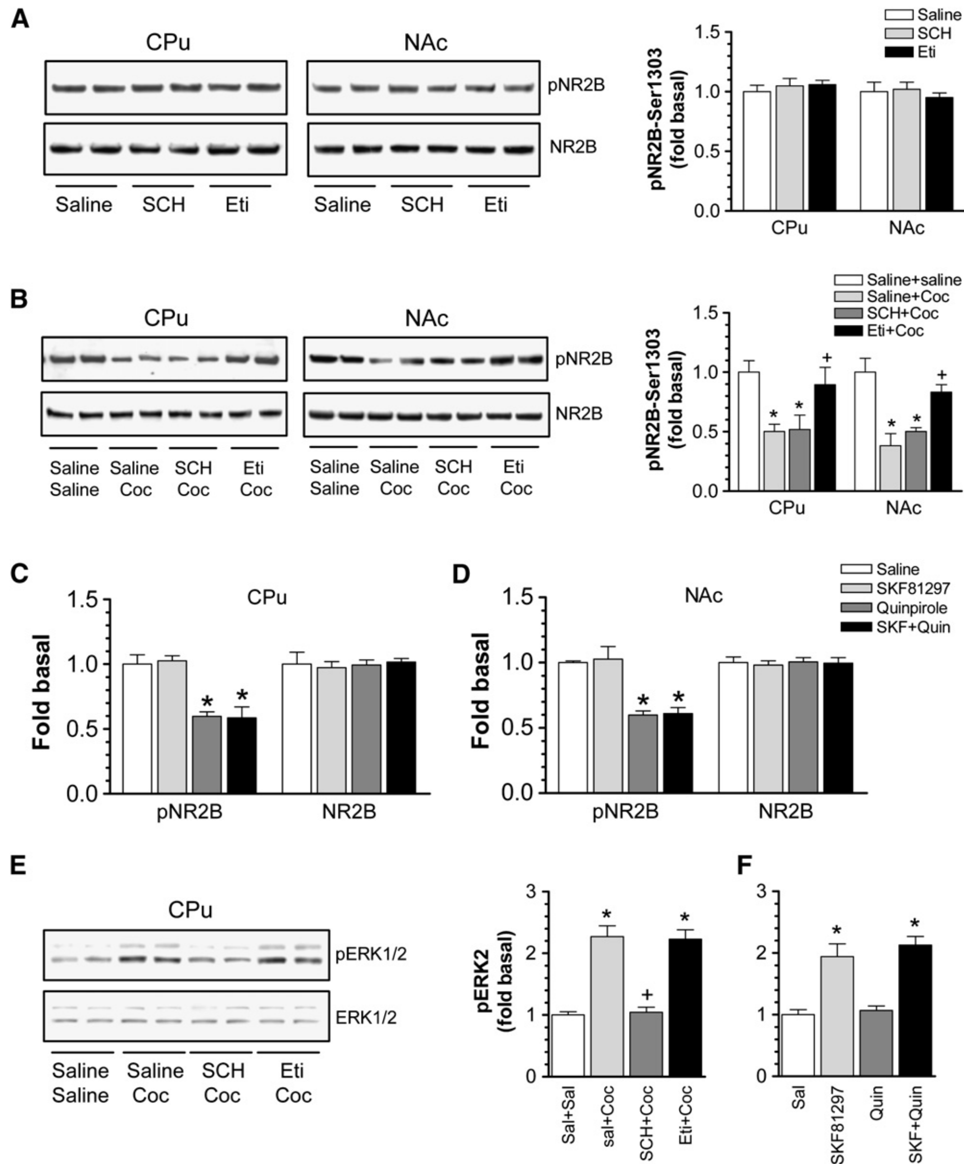

Figure 2. Activation of D2Rs Mediates the Cocaine Inhibition of NR2B-Ser1303 Phosphorylation in the CPu and NAc

(A) SCH23390 (SCH) or eticlopride (Eti) did not affect basal levels of pNR2B-Ser1303 and NR2B. Rats were given a single dose of SCH23390 (0.1 mg/kg, i.p.) or eticlopride (0.5 mg/kg, i.p.) and were sacrificed 30 min after drug injection. (B) Eticlopride, but not SCH23390, blocked the cocaine-induced decreases in pNR2B-Ser1303. (C and D) Quinpirole (Quin), but not SKF81297 (SKF), reduced pNR2B-Ser1303 levels. (E) SCH23390, but not eticlopride, blocked the cocaine-stimulated ERK1/2 phosphorylation in the CPu. (F) SKF81297, but not quinpirole, increased ERK1/2 phosphorylation in the CPu. In (B) and (E), SCH23390 (0.1 mg/kg, i.p.) or eticlopride (0.5 mg/kg, i.p.) was injected 15 min prior to an i.p. injection of saline or cocaine (40 mg/kg), and rats were sacrificed 30 min after cocaine injection. In (C), (D), and (F), rats were given a single dose of SKF81297 (1 mg/kg, i.p.) or quinpirole (1 mg/kg, i.p.) or a combination of the two agonists and were sacrificed 30 min after drug injection. Representative immunoblots are shown to the left of the quantified data of pNR2B-Ser1303 (A and B) or pERK2 (E). Data are presented as means ± SEM for three to six experiments. *$p < 0.05$ versus saline + saline (B and E) or saline (C, D, and F). $^{+}p < 0.05$ versus saline + cocaine.

(Figure 2B). In contrast, eticlopride blocked the cocaine inhibition of NR2B phosphorylation indistinguishably in the CPu and NAc (Figure 2B). To control the selectivity and effectiveness of the two antagonists in blocking their targets, the effect of these antagonists on a D1-dependent and D2-independent event, phosphorylation of extracellular signal-regulated kinase 1/2 (ERK1/2) in the striatum following acute cocaine stimulation (Valjent et al., 2000; Zhang et al., 2004) was tested in the same samples. We found that SCH23390 completely blocked, whereas eticlopride had no effect on, the cocaine-stimulated ERK1/2 phosphorylation in the CPu (Figure 2E), as opposed to their effects on the cocaine-induced inhibition of NR2B phosphorylation. These data validate the selectivity of these antagonists and thereby support a model in which selective activation of D2Rs mediates the inhibitory effect of cocaine on NR2B phosphorylation.

We next tested whether D1R or D2R activation with their selective agonists affects Ser1303 phosphorylation. Injection of the full D1R agonist SKF81297 (1 mg/kg, i.p.) alone did not change basal levels of pNR2B-Ser1303

in the CPu (Figure 2C) and NAc (Figure 2D). In contrast, the D2R agonist quinpirole (1 mg/kg, i.p.) alone markedly reduced pNR2B-Ser1303 levels in the striatum (Figures 2C and 2D) without changing the total amount of NR2B (Figures 2C and 2D). Coadministration of these two agonists produced a similar result as that observed after injection of quinpirole alone (Figures 2C and 2D). In addition, SKF81297 increased, whereas quinpirole did not alter, basal levels of phosphorylated ERK1/2 proteins in the CPu (Figure 2F). Thus, an enhanced dopaminergic tone on D2Rs rather than D1Rs suppresses Ser1303 phosphorylation.

D2Rs and NR2B Subunits Are Coclustered in Striatal PSD

Ultrastructural studies found the D2R existent in the post- and perisynaptic membrane of corticostriatal axospinous glutamatergic synapses in the rat striatum (Hersch et al., 1995; Wang and Pickel, 2002). We then extended these morphological observations to a biochemical analysis in the subcellular PSD fraction isolated from the striatum for investigating the presence of D2Rs in the PSD and the physical association of D2Rs with NR2B. The immunoblot with an anti-D2R antibody revealed a predominant specific band of ~70 kDa and a much lighter band of ~50 kDa (Wang and Pickel, 2002) in the PSD and P2 fractions, which were blocked by preabsorption of the antibody with an immunogen peptide (Figure 3A). The specific bands mostly enriched in the PSD and P2 fractions were also seen for the NR1 subunit, the NR2B subunit, and CaMKIIα, three known PSD constituents (Figure 3B). The purity of the PSD fraction was confirmed by the lack of immunoreactivity for PKCε, a known PKC isozyme present exclusively in the presynaptic compartment (Figure 3B). To determine whether D2Rs and NR2B interact with each other in the PSD, coimmunoprecipitation studies were performed using the PSD fraction. A clear and specific D2R band presented in NR2B precipitates (Lane 4 in Figure 3C). In a reverse coimmunoprecipitation, a specific NR2B band was also detected in D2R precipitates (Lane 4 in Figure 3D). These specific bands did not appear when either the precipitating antibody was omitted (Lane 2) or when an irrelevant IgG was used (Lane 3). In contrast, D1R immunoreactivity was not detectable in either NR2B (Figure 3C) or D2R precipitates (Figure 3D), and a specific NR2B or D2R band was not present in D1R precipitates, even though D1Rs could be precipitated from striatal PSD fraction (data not shown). These results reveal a constitutive formation of a heteroreceptor complex containing D2Rs and NR2B in the PSD microdomain of striatal neurons in vivo. Similarly, a D2R band was seen in NR2B precipitates in the PSD fraction from the hippocampus and the frontal cortex (Figure S3), indicating an existence of the D2R-NR2B interaction in broad areas.

To identify a specific D2R region responsible for the D2R-NR2B complex formation, glutathione-S-transferase (GST) fusion proteins were prepared from sequences within two intracellular domains of D2Rs: the carboxyl tail ($D2R_{CT}$) and the third intracellular loop ($D2R_{IL3}$). The $D2R_{IL3}$ fragment was based on the long, instead of the short, form of D2Rs because D2R-long is preferentially involved in postsynaptic signaling (Usiello et al., 2000; Lindgren et al., 2003). Using a pull-down assay, the ability of GST-$D2R_{CT}$ and GST-$D2R_{IL3}$ fusion proteins to recognize and precipitate NR2B from solubilized striatal tissue (P2) was tested. We found that GST-$D2R_{IL3}$, but not GST-$D2R_{CT}$ or GST alone, precipitated NR2B (Figure 3E). GST alone and the two GST fusion proteins did not precipitate D1Rs (Figure 3F). Thus, the prime D2R region for D2Rs to complex with NR2B is restricted to the $D2R_{IL3}$ region. Similarly, using GST-$NR2B_{CT}$ and GST-NR1-$1a_{CT}$ fusion proteins, we found that the former, but not the latter or GST alone, precipitated D2Rs (Figure 3G). GST-NR1-$1a_{CT}$ could only precipitate D1Rs (Figure 3H) as reported previously (Lee et al., 2002). Thus, NR2B interacts with D2Rs through its carboxyl tail. In contrast to D2Rs, D3Rs did not seem to interact with NR2B because GST-$D3R_{IL2}$ and GST-$D3R_{IL3}$ did not precipitate NR2B (Figure S4).

Direct Protein-Protein Interaction between D2Rs and NR2B

To define whether the D2R-NR2B interaction is direct and to reveal the region of $D2R_{IL3}$ involved in the interaction, we conducted blot overlay and in vitro binding assays using purified GST-$D2R_{IL3}$ and $NR2B_{CT}$ proteins. The direct interaction of $NR2B_{CT}$ with $D2R_{IL3}$ was demonstrated in blot overlay experiments, in which $NR2B_{CT}$ bound with GST-$D2R_{IL3}$ but not GST-$D3R_{IL3}$ (Figure 3J), whereas $D2R_{IL3}$ bound with GST-$NR2B_{CT}$ but not GST-NR1-$1a_{CT}$ (Figure 3K). Furthermore, $NR2B_{CT}$ selectively bound with GST-$D2R_{IL3\text{-}1}$, but not GST-$D2R_{IL3\text{-}2}$ (Figures 3I and 3J), indicating that the N-terminal 32 amino acid residue (I210-K241) of $D2R_{IL3}$ is a critical binding region to $NR2B_{CT}$. These results were further confirmed in in vitro binding assays (Figure 3L). GST-$D2R_{IL3}$ and GST-$D2R_{IL3\text{-}1}$, but not GST-$D2R_{IL3\text{-}2}$, GST-$D3R_{IL3}$, or GST alone, precipitated $NR2B_{CT}$ in these assays. All blots were probed in parallel with a GST antibody to assure equivalent protein loading (data not shown).

A sufficient binding motif within the first 32 residues of $D2R_{IL3}$ was further identified in competition assays. As shown in Figures 3M and 3N, purified peptides that contain a motif of ten residues (TKRSSRAFRA), including $D2R_{IL3}$-P1, -P2, -P3, and -P5 peptides, blocked the $D2R_{IL3}$-$NR2B_{CT}$ binding, whereas the $D2R_{IL3}$-P4 peptide lacking this motif had no effect. The $D2R_{IL3}$-P6 peptide (a sequence-scrambled control of $D2R_{IL3}$-P5) did not alter the $D2R_{IL3}$-$NR2B_{CT}$ binding, supporting the idea that the binding is sequence-specific. Noticeably, the binding motif identified here represents a distinct region within the first 32 $D2R_{IL3}$ amino acids that is conserved in different species and is adjacent to a calmodulin binding domain (I210-V223) reported previously (Bofill-Cardona et al., 2000). However, $D2R_{IL3}$-P5 is believed to have no effect on the $D2R_{IL3}$-calmodulin binding because the truncated $D2R_{IL3}$ peptides encompassing $D2R_{IL3}$-P5 did not bind to calmodulin (Bofill-Cardona et al., 2000).

Cocaine Facilitates the D2R-NR2B Association

More coimmunoprecipitation studies were conducted to assess changes of the D2R-NR2B association in striatal extracts (P2) in response to cocaine stimulation in vivo. Cocaine (30 mg/kg, 30 min) increased the level of D2Rs in NR2B precipitates (Figure 4A) and the level of NR2B

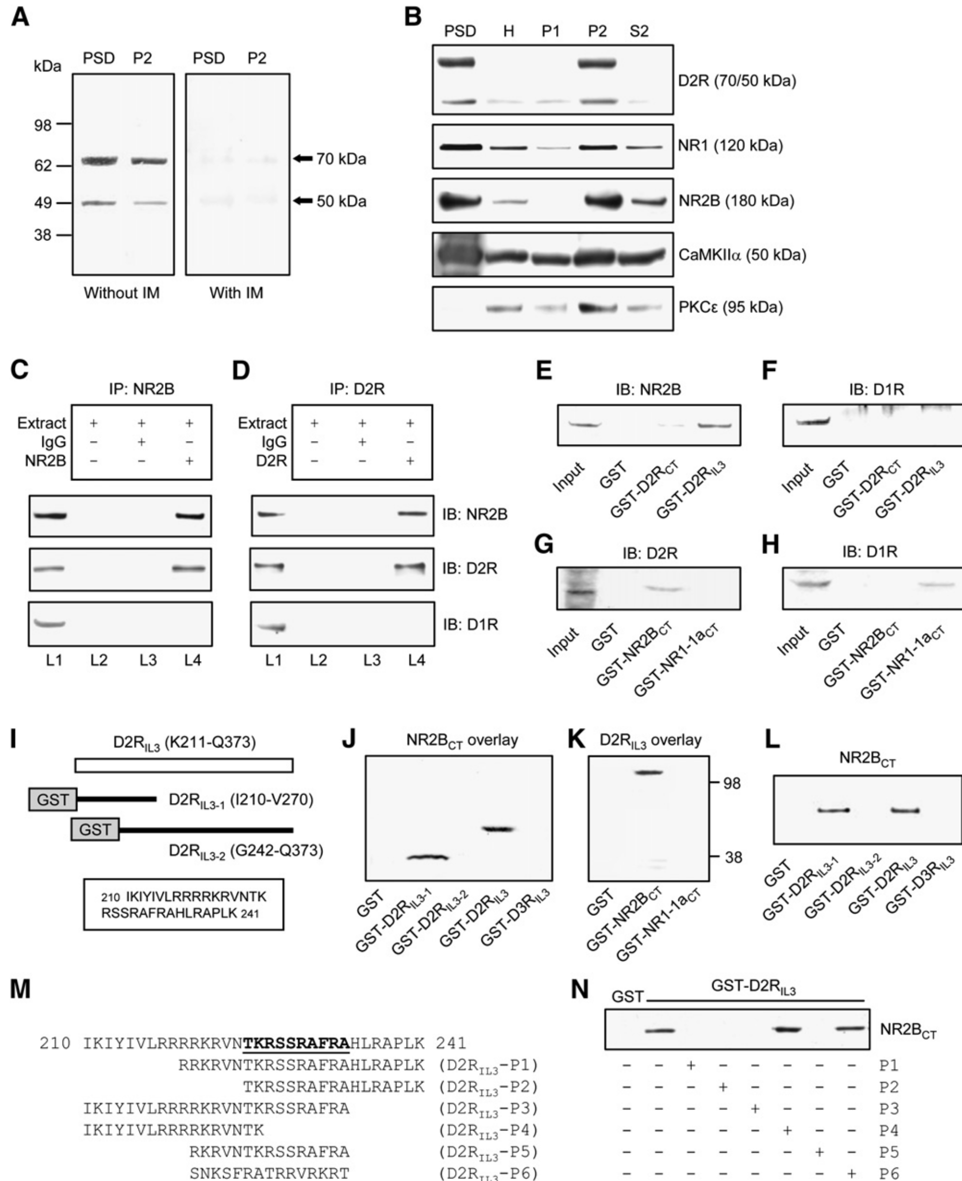

Figure 3. Association of D2Rs and NR2B in Striatal Neurons

(A) Immunoblots carried out in the PSD and P2 fractions using an anti-D2R antibody with or without an immunogen (IM) peptide: a 28 amino acid fragment (284–311, LSSTSPPERTRYSPIPPSHHQLTLPDPS) within $D2R_{IL3}$.

(B) Immunoblots carried out in the different fractions of striatal protein extractions. Proteins were loaded at 5 μg per lane.

(C and D) Coimmunoprecipitation (IP) of NR2B and D2Rs in striatal PSD. Immunoblot (IB) results (L4) showed that NR2B coprecipitated with D2Rs (C) and vice versa (D). D1Rs coprecipitated with neither NR2B nor D2Rs. Lane 1 represents non-IP samples and no specific band was present in lanes 2 and 3 due to the lack of immunoprecipitating antibodies in samples (L2) and the use of an irrelevant IgG (L3).

(E–H) Pull-down assays with GST or GST fusion proteins from solubilized rat striatal tissue.

(I) Mapping of the $NR2B_{CT}$ binding region in $D2R_{IL3}$. Two GST fusion proteins containing $D2R_{IL3}$ portions as indicated were generated and purified.

(J and K) Blot overlay assays showing $NR2B_{CT}$ binding to GST-$D2R_{IL3\text{-}1}$ and GST-$D2R_{IL3}$ (J) and $D2R_{IL3}$ binding to GST-$NR2B_{CT}$ (K).

(L) In vitro binding assays showing $NR2B_{CT}$ binding to GST-$D2R_{IL3\text{-}1}$ and GST-$D2R_{IL3}$.

(M) The NR2B binding motif in $D2R_{IL3}$. The primary sequence of the first 32 amino acids of $D2R_{IL3}$ is shown. Underlined and bold letters indicate the potential $NR2B_{CT}$ binding motif.

(N) In vitro binding assays showing the blockade of $NR2B_{CT}$-$D2R_{IL3}$ binding upon the addition of $D2R_{IL3}$ peptides (P1, P2, P3, and P5).

in D2R precipitates (Figure 4B). In rats pretreated with eticlopride (0.5 mg/kg), cocaine no longer induced a significant increase in the amount of D2Rs in NR2B precipitates (Figure 4C). In contrast, SCH23390 (0.1 mg/kg) did not alter the ability of cocaine to increase D2R levels in NR2B precipitates (Figure 4D). These data indicate a dynamic elevation of the interaction between D2Rs and NR2B following selective activation of D2Rs by cocaine. The effect of cocaine seems to be region-specific because no change in the D2R-NR2B coimmunoprecipitation was found in the hippocampus and the frontal cortex following cocaine administration (Figure S5).

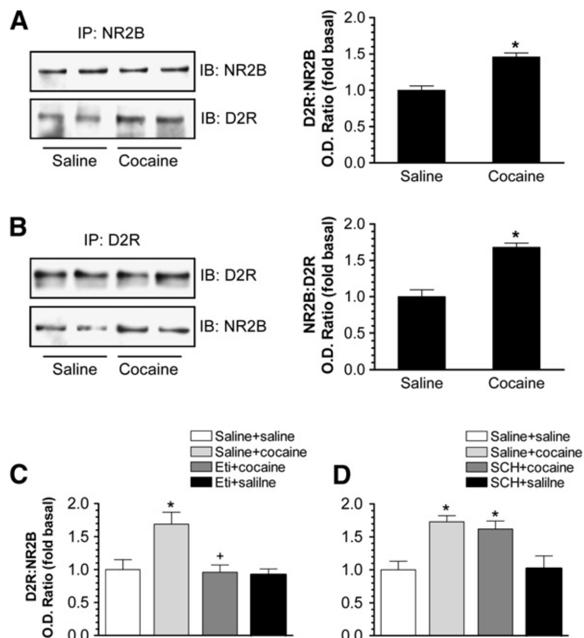

Figure 4. Coimmunoprecipitation of D2Rs with NR2B in Striatal Neurons Following Cocaine Stimulation

(A and B) Cocaine increased the association of D2Rs with NR2B. Immunoblots were performed on NR2B or D2R immunoprecipitates. Saline or cocaine (30 mg/kg, i.p.) was given 30 min before sacrifice. Representative immunoblots are shown to the left of the quantified data in terms of optical density ratios. Data are presented as means ± SEM for four to six experiments. (C and D) Effects of eticlopride (C) and SCH23390 (D) on the cocaine-induced formation of the D2R-NR2B complex. Eticlopride, but not SCH23390, blocked an increase in the D2R level in NR2B precipitates. Eticlopride (0.5 mg/kg, i.p.) or SCH23390 (0.1 mg/kg, i.p.) was injected 15 min prior to an i.p. injection of saline or cocaine (30 mg/kg), and rats were sacrificed 30 min after cocaine injection. *$p < 0.05$ versus saline (A and B) or saline + saline (C). $^{+}p < 0.05$ versus saline + cocaine.

The Role of CaMKII in D2R-Dependent Inhibition of Ser1303 Phosphorylation

CaMKII is an abundant kinase in the PSD (Kelly et al., 1984). This kinase and PKC drive NR2B Ser1303 phosphorylation in hippocampal neurons or *Xenopus* oocytes (Omkumar et al., 1996; Liao et al., 2001). To identify the kinase(s) that can phosphorylate Ser1303 in the native NR2B in striatal neurons, dephosphorylated striatal homogenates were incubated in the phosphorylation mixture, which contained recombinant human PKA, PKC, or CaMKIV, or rat brain CaMKII. PKA and CaMKIV failed to alter Ser1303 phosphorylation and PKC slightly increased it (Figure 5A). Strikingly, CaMKII induced a nearly 3-fold increase in Ser1303 phosphorylation (Figure 5A). The CaMKII effect was blocked by the CaMKII inhibitor KN93 (20 μM)—but not its inactive analog KN92 (Figure 5B)—and by a CaMKII peptide inhibitor (Chang et al., 1998) at 100 nM (data not shown). These results reveal that in striatal neurons CaMKII is a key kinase driving NR2B phosphorylation at Ser1303.

We then examined changes in CaMKII activity in striatal tissue in response to cocaine stimulation. Acute cocaine injection (30 mg/kg) induced a rapid and transient reduction of CaMKII activity (Figure 5C), which corresponded well with the kinetic of reduced Ser1303 phosphorylation. The reduction was sensitive to the D2R antagonist eticlopride (Figure 5D), but not the D1R antagonist SCH23390. In an effort to detect changes in a known direct association of CaMKII with NR2B (Gardoni et al., 1998), we found that cocaine decreased the amount of CaMKIIα and phospho-CaMKIIα-Thr^{286} in NR2B precipitates (Figure 5E). In a reverse immunoprecipitation, a lower level of NR2B was also seen in CaMKIIα precipitates. Thus, cocaine seems to reduce CaMKII-NR2B binding and CaMKII activity, which may account for the cocaine inhibition of Ser1303 phosphorylation.

D2Rs Inhibit NMDAR-Mediated Currents

To determine whether D2Rs can modulate NMDAR function, we recorded whole-cell NMDAR-mediated currents in acutely dissociated, medium-sized striatal neurons. We found that quinpirole at 10, but not 0.1, μM significantly reduced NMDAR currents in 13 out of 21 neurons surveyed (Figures 6A and 6B). The reduction of NMDAR currents appears to be reversible since reduced NMDAR currents showed a trend toward recovery after quinpirole was washed off (Figure 6B). The quinpirole effect was mediated by D2Rs because bath perfusion of eticlopride (1 μM) blocked the depression of NMDAR currents induced by quinpirole in all neurons tested (Figures 6C and 6D, n = 16). A critical role of the identified direct protein-protein interaction between D2Rs and NR2B in the modulation of NMDAR currents by D2Rs is illustrated in Figures 6E and 6F. Intracellular application of the $D2R_{IL3}$-P5 peptide (20 μM) prevented the inhibition of NMDAR currents induced by quinpirole (n = 20). In contrast, the control $D2R_{IL3}$-P6 peptide had no such effect, and quinpirole (10 μM) still significantly reduced NMDAR current in 14 out of 27 cells recorded.

The Role of D2R-NR2B Interaction in Behavioral Responsiveness to Cocaine

We extended our molecular observations to behavioral experiments to investigate whether the cocaine-regulated D2R-NR2B interaction can translate to the modulation of the regulation of behavioral responsiveness to cocaine. Cocaine is well known to require activation of both D1Rs and D2Rs, followed by activation of the direct (striatonigral) pathway and suppression of the indirect (striatopallidal) pathway, respectively, to increase the outflow of the basal ganglia, which leads to motor stimulation. We then speculate that, following cocaine stimulation, concomitant activation of D2Rs and inhibition of NR2B-containing NMDARs occurs in D2R/NR2B-bearing neurons through the D2R-NR2B integration, and that this process is required for synergistically suppressing the indirect pathway. Consistent with this model, in open field locomotor activity assays, the D2R agonist quinpirole (1 mg/kg) augmented behavioral responses to cocaine (15 mg/kg, Figure 7A). Interestingly, the systemically active NR2B selective antagonist RO25-6981 (IC50 of 9 nM and 52 μM for NR1/NR2B and NR1/NR2A, respectively) (Fischer et al., 1997), which itself did not alter spontaneous motor activity (Figure 7B), mimicked the effect of quinpirole in eliciting significantly higher behavioral responses to cocaine as measured by horizontal activity (Figure 7C) and stereotypy (Figure 7D). The latter was characterized by

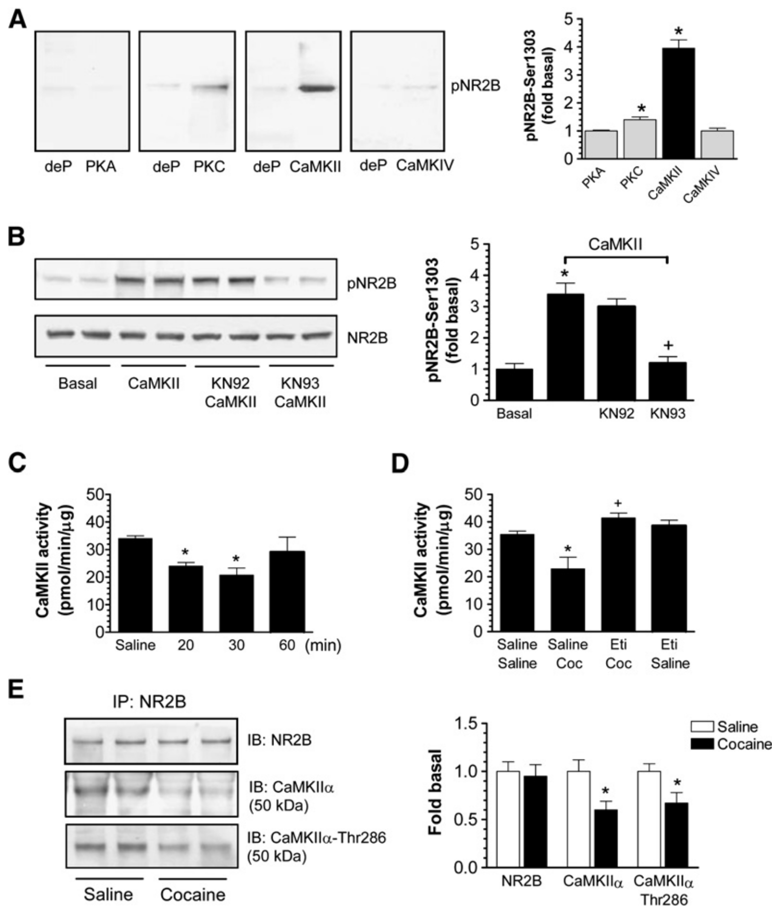

Figure 5. Phosphorylation of NR2B at Ser1303 by CaMKII

(A) Phosphorylation of Ser1303 by protein kinases. An aliquot (30 μg) of striatal homogenates was subjected to dephosphorylating conditions (deP) or to dephosphorylating conditions followed by phosphorylation by PKA, PKC, CaMKII, or CaMKIV at 50 ng (5 min, 30°C). (B) The CaMKII inhibitor blocked the CaMKII-regulated Ser1303 phosphorylation. Following the dephosphorylation of striatal homogenates, KN93 or KN92 at 20 μM in combination with CaMKII (50 ng) was added into the phosphorylation mixture for a 5 min incubation (30°C). (C) Effects of cocaine on CaMKII activity assayed on synaptosome-enriched fractions of striatal tissue. Rats were injected with cocaine (30 mg/kg, i.p.) and sacrificed at indicated time points after cocaine injection. (D) Eticlopride blocked the reduction of CaMKII activity by cocaine. Eticlopride (0.5 mg/kg, i.p.) was injected 15 min prior to an i.p. injection of saline or cocaine (30 mg/kg) and rats were sacrificed 30 min after cocaine injection. (E) Coimmunoprecipitation of NR2B with CaMKIIα and phospho-CaMKIIα-Thr^{286} in striatal tissue (P2) from rats treated with saline or cocaine (30 mg/kg, i.p., 30 min before tissue collection). Immunoblots were performed on NR2B precipitates. Representative immunoblots are shown to the left of the quantified data (A, B, and E). Data are presented as means ± SEM from five to six experiments (A and B) or five to eight animals per group (C–E). $^{*}p < 0.05$ versus deP (A), basal levels (B), or saline (C–E). $^{+}p < 0.05$ versus CaMKII alone (B) or saline + cocaine (D).

intensive sniffing and biting. Another NR2B selective antagonist, ifenprodil (1–2 mg/kg), produced the same effect (Figure S6A). Quinpirole and RO25-6981, when coadministered at their subthreshold doses, at which they did not significantly alter the cocaine effect, significantly enhanced a locomotor activity induced by cocaine (Figure 7E). Thus, D2R activation and NR2B inhibition could synergistically augment behavioral responsiveness to cocaine. The motor stimulation from cocaine alone or in combination with RO25-6981 requires D2R activation because the D2R antagonist eticlopride (0.5 mg/kg) blocked motor activity induced by cocaine or cocaine + RO25-6981 (Figure 7F). To determine whether the effect of systemic RO25-6981 primarily occurs in the local striatum, a microinjection study targeting the NAc or the CPu was performed in chronically prepared and freely moving rats. Microinjection of this agent into the NAc produced the same effect as that observed following systemic injections (Figure 7G). So did microinjection of this agent into the CPu (Figure S6B). In sharp contrast to the NR2B antagonist, the relatively NR2A selective antagonist NVP-AAM077 (Auberson et al., 2002; but Neyton and Paoletti, 2006) failed to augment a behavioral response to cocaine when given locally (Figure 7G) or systemically (Figure 7I). In fact, NVP-AAM077 at 2 mg/kg significantly reduced spontaneous and cocaine-stimulated motor activity (Figure 7I). These data support the notion that the D2R-NR2B interaction synergistically inhibits the indirect pathway and thereby controls behavioral responsiveness to cocaine.

To define the direct role of the D2R-NR2B interaction, we synthesized systemically active and cell-permeable Tat-fusion peptides (Tat-$D2R_{IL3}$-P5, with demonstrated ability to disrupt the D2R-NR2B binding, and its control, Tat-$D2R_{IL3}$-P6). Using fluorescently tagged peptides (FITC-Tat-$D2R_{IL3}$-P5), we detected the presence of these peptides in striatal neurons after a single intravenous (i.v.) injection (3 nmol/g). Striatal concentration of the peptide increased in a time-dependent manner and peaked 90 min after injection (Figure 8A). Pretreatment with the interference peptide Tat-$D2R_{IL3}$-P5 (3 nmol/g, i.v., 90 min before cocaine) prevented the elevation of the D2R-NR2B interaction induced by cocaine (Figure 8B). Tat-$D2R_{IL3}$-P5 also reversed the reduction of the CaMKII-NR2B interaction (Figure 8C) and Ser1303 phosphorylation (Figure 8D) induced by cocaine. Pretreatment with the control peptide (Tat-$D2R_{IL3}$-P6) had no such effects (Figures 8B–8D). Moreover, Tat-$D2R_{IL3}$-P5, but not Tat-$D2R_{IL3}$-P6, markedly attenuated cocaine-stimulated horizontal activity (Figure 8E) and stereotypy (Figure 8F). The two peptides had no effect on the basal CaMKII-NR2B binding and Ser1303 phosphorylation, although Tat-$D2R_{IL3}$-P5 reduced the basal D2R-NR2B interaction to 71.4% of control ($p < 0.05$). No noticeable behavioral side effects were observed with peptide treatment. These results provide strong evidence supporting a critical role of the D2R-NR2B interaction in mediating cocaine's effect on CaMKII-NR2B binding and Ser1303 phosphorylation and in constructing a full-scale motor response to cocaine.

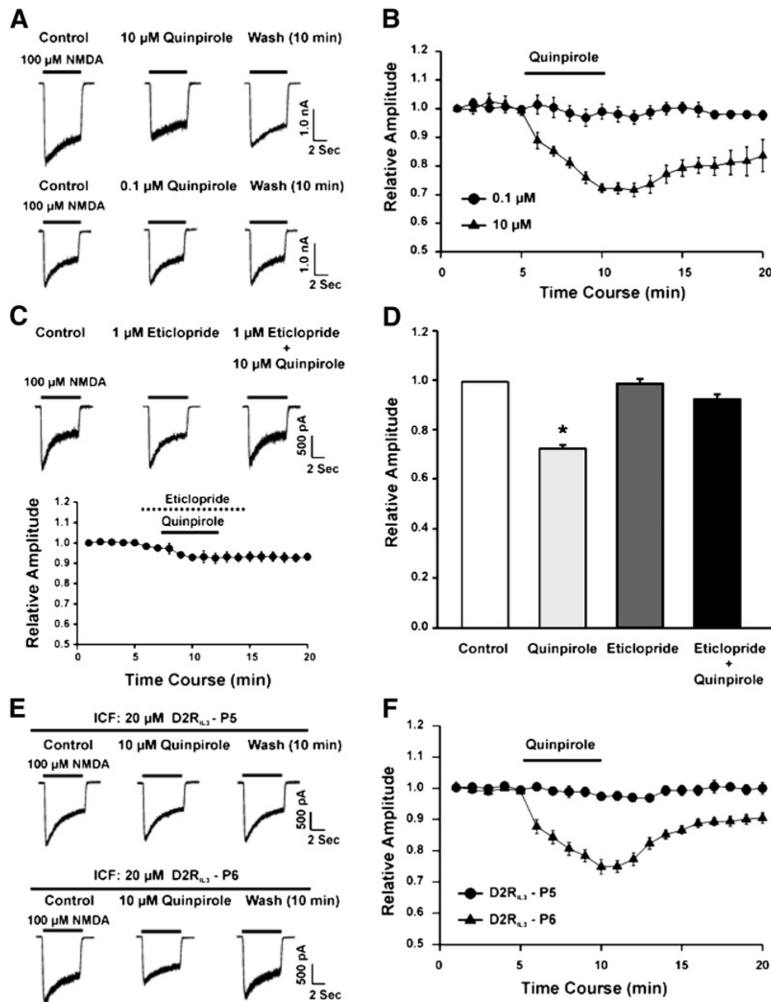

Figure 6. Activation of D2Rs Inhibits NMDAR-Mediated Currents in Acutely Dissociated Striatal Neurons

(A) Representative traces indicating that bath application of the D2R agonist quinpirole at 10 μM (upper traces), but not 0.1 μM (lower traces), reduced NMDAR currents.

(B) Time courses of the quinpirole effect on NMDAR currents.

(C) Representative traces elucidating the blockade of the quinpirole-induced reduction of NMDAR currents by bath application of the D2R antagonist eticlopride (1 μM). A time course graph is shown below the representative traces.

(D) Summary data showing the inhibition of NMDAR currents by quinpirole (10 μM) in the absence and presence of eticlopride (1 μM).

(E and F) Application of $D2R_{IL3}$-P5, but not $D2R_{IL3}$-P6, peptide (20 μM) in intracellular fluid (ICF) blocked the quinpirole inhibition of NMDAR currents. Data are presented as means ± SEM (n = 14 to 27). *$p < 0.05$ versus control.

Discussion

Both dopamine and glutamate receptors are densely expressed in striatal neurons. Active interactions between them are believed to occur at the receptor level. Indeed, the results obtained from this study reveal the direct binding between the third intracellular loop of D2Rs and the C-terminal region of NR2B. This interaction is responsive to cocaine stimulation, and the upregulated interaction seems to be involved in the reduction of both CaMKII binding to NR2B and NR2B Ser1303 phosphorylation. Electrophysiological studies provide evidence supporting D2R inhibition of NMDAR currents through interactions with NR2B. Behaviorally, the D2R-NR2B interaction is critical for behavioral responses to acute cocaine administration.

Dopamine-Glutamate Interactions Control Psychostimulant Actions

The dopamine-glutamate interaction is a key factor in determining stimulant actions. Recent studies focus on molecular mechanisms underlying the interaction. Available data show that dopamine stimulation can regulate total levels or trafficking of NMDARs, AMPA receptors, and glutamate receptor anchoring proteins, such as PSD-95 and Homer, in striatal neurons (Dunah et al., 2004; Szumlinski et al., 2004; Yao et al., 2004; Boudreau and Wolf, 2005). Both dopamine and glutamate also regulate the phosphorylation state of dopamine- and cAMP-regulated phosphoprotein with molecular weight 32 kDa (DARPP-32) in striatal neurons (reviewed in Svenningsson et al., 2005). Moreover, a direct protein-protein coupling has been shown to enable functional crosstalk between D1Rs and the NR1 subunit (Lee et al., 2002; Fiorentini et al., 2003). All these models of dopamine-glutamate interactions are believed to contribute to the development of various forms of synaptic and behavioral plasticity in response to stimulants. The results from the present study add another dopamine-glutamate interaction model in which D2Rs and NR2B functionally crosstalk to control neuronal and behavioral responses to cocaine.

Direct D2R-NR2B Interactions in Striatal Neurons

A noteworthy finding in this study is the direct interaction between D2Rs and NR2B in striatal neurons. This interaction is responsive to enhanced dopaminergic inputs in vivo by cocaine and is believed to occur postsynaptically because the interaction was revealed in the isolated PSD microdomain and modulated NMDAR currents in dissociated striatal neurons. The specific population(s) of striatal neurons that

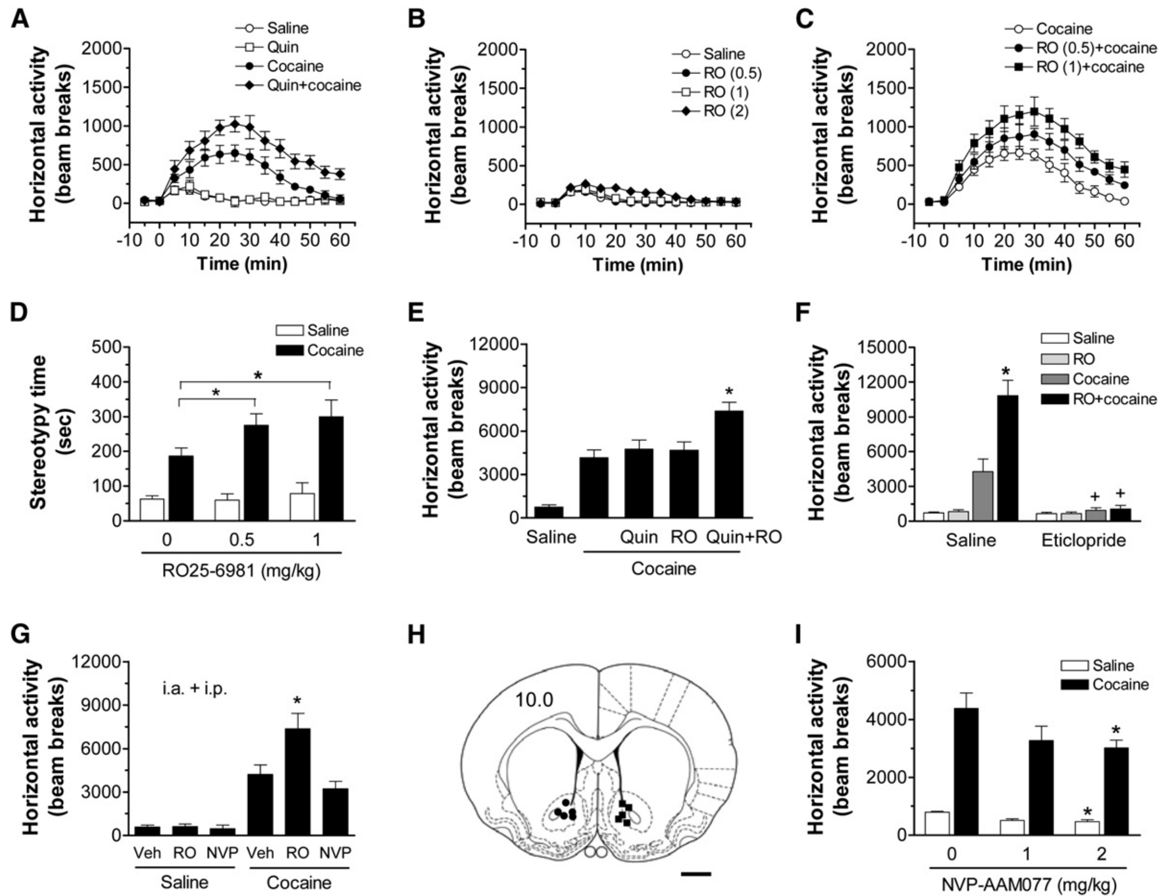

Figure 7. A Synergistic Effect of the D2R Agonist and the NR2B Antagonist on Behavioral Responses to Cocaine in the Open Field

(A) Coadministration of quinpirole (Quin, 1 mg/kg, i.p.) augmented cocaine-stimulated horizontal activity. (B) Effects of the NR2B-NMDAR selective antagonist RO25-6981 (RO) at 0.5, 1, or 2 mg/kg (i.p.) on spontaneous motor activity. (C and D) Coadministration of RO25-6981 (0.5 and 1 mg/kg, i.p.) augmented cocaine-stimulated horizontal activity (C) and stereotypy time (D). (E) Quinpirole and RO25-6981 at their subthreshold doses (0.25 mg/kg for quinpirole and 0.1 mg/kg for RO25-6981, i.p.) synergistically augmented cocaine-stimulated horizontal activity. (F) Effects of eticlopride (0.5 mg/kg, i.p.) on horizontal activity induced by cocaine or RO25-6981 (1 mg/kg, i.p.) + cocaine. Saline or eticlopride was given 15 min prior to cocaine, RO25-6981, or cocaine + RO25-6981. (G) Intra-accumbal (i.a.) injection of RO25-6981, but not the NR2A-NMDAR selective antagonist NVP-AAM077 (NVP), augmented cocaine-stimulated horizontal activity. RO25-6981 (2.5 μg/0.4 μl/side) or NVP-AAM077 (2.5 μg/0.4 μl/side) was injected 5 min prior to systemic injection of cocaine. (H) Locations of microinjection sites within the nucleus accumbens. Representative sites are illustrated on only one side of the slice (interaural distance = 10.0 mm) for the bilateral injections of vehicle (filled circles) and RO25-6981 (filled squares) in cocaine-treated rats used in (G). Scale bar, 1 mm. (I) Effects of coadministration of NVP-AAM077 (1 or 2 mg/kg, i.p.) on cocaine-stimulated horizontal activity. Cocaine was injected i.p. at 15 mg/kg in all studies. Data are expressed as means ± SEM of behavioral activity measured for 60 (A–C) or 40 (D–G and I) min after cocaine injection (n = 4 to 7 per group). *$p < 0.05$ versus cocaine (D–G) alone or the corresponding values in rats without NVP-AAM077 treatment (I). $^{+}p < 0.05$ versus the corresponding values in rats treated with saline (F).

coexpress(es) D2Rs and NR2B may host this interaction. All striatopallidal projection neurons contain a high level of D2Rs (Surmeier et al., 1996; Aizman et al., 2000). The physiological effect of the interaction (i.e., D2R inhibition of NMDAR currents) was seen in about half of medium-sized spiny neurons. Thus, striatopallidal efferent neurons likely represent a main subpopulation of striatal neurons for this event, although the experiments in this study did not exclude the possibility that a small portion of striatonigral output neurons that coexpress a low level of D2Rs (Aizman et al., 2000) or D2R-containing cholinergic interneurons may also host this interaction. It is possible that D2Rs are strategically positioned in the NR2B-enriched PSD of excitatory synapses for a direct interaction of two receptors. Ultrastructural observations seem to support this idea. D2Rs are enriched in dendritic spine shafts and heads that are contacted by corticostriatal glutamatergic afferents to form axospinous asymmetric synapses throughout the striatum (Hersch et al., 1995; Yung and Bolam, 2000). A dense and widespread membrane localization of D2Rs is present outside nigrostriatal dopaminergic symmetric synapses (Graybiel et al., 1981), making it possible for them to respond to dopamine that has overspilled from its synaptic cleft (Sesack et al., 2004) or to dopamine extrasynaptically derived from volume transmission (Hersch et al., 1995). Together, the data obtained in this study support a synaptic model for a direct and dynamic receptor-receptor interaction between the two dominant receptors in the striatum. This interaction may integrate with other $D2R_{IL3}$ binding partners identified previously (Bofill-Cardona et al., 2000; Bibb, 2005) to control the cellular response to converging dopamine and glutamate inputs.

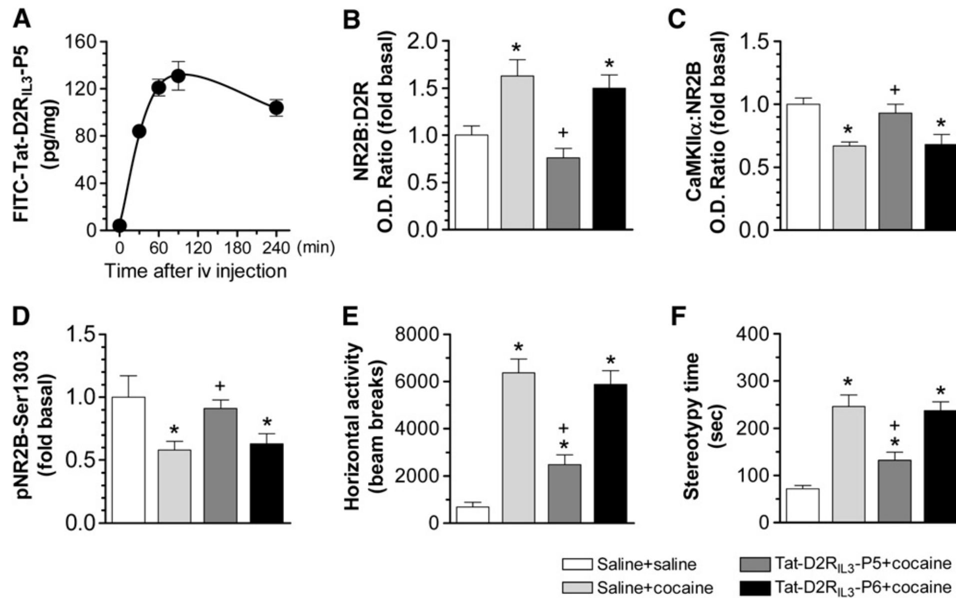

Figure 8. Intravenous Administration of the Interference Peptide Tat-D2R$_{IL3}$-P5 Altered the Cocaine-Stimulated Cellular and Motor Responses

(A) Transduction of Tat-D2R$_{IL3}$-P5 peptides in the rat striatum. After FITC-Tat-D2R$_{IL3}$-P5 injection (3 nmol/g, i.v.), animals were perfused with saline and the concentrations of peptide in striatal tissue were determined at indicated time points.

(B and C) Summary data from coimmunoprecipitation showing the NR2B level in striatal D2R precipitates (B) and the CaMKIIα level in striatal NR2B precipitates (C).

(D) Summary data from immunoblots showing effects of cocaine on NR2B Ser1303 phosphorylation in the striatum of rats pretreated with Tat-D2R$_{IL3}$-P5 or Tat-D2R$_{IL3}$-P6.

(E and F) Effects of cocaine on horizontal activity (E) and stereotypy (F) in rats pretreated with Tat-D2R$_{IL3}$-P5 or Tat-D2R$_{IL3}$-P6. Tat peptides were given at 3 nmol/g (i.v.) 90 min prior to cocaine (30 mg/kg, i.p.) or saline and rats were sacrificed 35 min after cocaine injection. Data are expressed as means ± SEM (n = 3 to 6 per group). $^{*}p < 0.05$ versus saline + saline. $^{+}p < 0.05$ versus saline + cocaine.

The Role of CaMKII in the Regulation of NR2B Phosphorylation in Response to Cocaine

CaMKII is known to play a significant role in synaptic plasticity (Soderling, 2000; Sheng and Kim, 2002). This role has been tightly related to its ability to regulate glutamate receptor phosphorylation. In hippocampal neurons, CaMKII acts as a prime kinase to catalyze constitutive NR2B phosphorylation at Ser1303 (Omkumar et al., 1996). Similarly, in striatal neurons, CaMKII is the most potent kinase in upregulating NR2B Ser1303 phosphorylation, based on observations in this study. In response to cocaine stimulation, CaMKII is also an essential element in sequential events leading to the D2R inhibition of NR2B phosphorylation. This was demonstrated by the findings that cocaine induced a D2R-dependent reduction of CaMKII activity in a time course corresponding to the kinetics of reduced Ser1303 phosphorylation and reduced the CaMKII binding to NR2B. Since the disruption of the D2R-NR2B binding with the Tat-D2R$_{IL3}$-P5 peptide blocked the cocaine-induced reduction of both CaMKII-NR2B binding and NR2B phosphorylation, the direct D2R-NR2B interaction contributes to these cocaine effects. It appears that the enhanced D2R-NR2B interaction after cocaine may disrupt the CaMKII-NR2B association. This results in the weakening of CaMKII influence over its specific phosphorylation site (Ser1303), leading to reduced Ser1303 phosphorylation.

Physiological Effects of the D2R-NR2B Interaction, a Synaptic Model for Dopamine-Glutamate Synergy

Whether the D2R-NR2B interaction modulates the excitability of NMDARs and determines behavioral responsiveness to psychostimulants is particularly intriguing. The traditional direct and indirect pathways in the basal ganglia originate from striatonigral and striatopallidal projection neurons, respectively. Synergistic interactions between striatonigral (stimulation) and striatopallidal (inhibition) neurons are required for motor responses to psychostimulants. It is known that dopamine and glutamate dynamically interact with each other to determine the outflow of the two pathways, but the underlying molecular mechanisms are unclear. The findings in this study suggest a mechanism which involves a direct receptor-receptor interaction. When this direct D2R-NR2B interaction primarily occurs in D2R-enriched striatopallidal output neurons, concurrent D2R activation and NR2B-NMDAR inhibition could take place through the D2R-NR2B coupling, which could then synergistically suppress the indirect pathway in response to cocaine. The suppression of the indirect pathway by this method cooperates with stimulation of the direct pathway to jointly determine a final output from the basal ganglia circuit. The data from the current electrophysiological and behavioral studies are remarkably consistent with this notion. Electrophysiologically, D2R activation inhibited NMDAR currents in medium efferent neurons,

similar to small reductions of NMDAR currents in some medium neurons in a previous report (Flores-Hernandez et al., 2002). The direct D2R-NR2B interaction is required for this inhibition, a mechanism in addition to an indirect inhibition of NMDAR currents in hippocampal neurons by D2Rs (Kotecha et al., 2002). Behaviorally, the NR2B antagonists mimicked the D2R agonist in augmenting cocaine-stimulated motor activity. Coadministration of the D2R agonist and the NR2B antagonist at their subthreshold doses synergistically potentiated the cocaine effect. More importantly, the disruption of D2R-NR2B binding severely impaired the ability of cocaine to produce a full-scale motor response. It is less likely that the NR2B-containing NMDAR in D1R-enriched striatonigral neurons contributes to these events because (1) D1Rs showed no association with NR2B in terms of direct receptor-receptor interaction (Lee et al., 2002; Fiorentini et al., 2003; this study); and (2) inhibition of NR2B-NMDARs in D1R-enriched neurons, if there is any, is more likely to counteract D1R stimulation of the direct pathway and thus attenuate motor stimulation. Together, the results from the current study appear to support a critical role of the D2R-NR2B interaction in suppressing the D2R-dependent indirect pathway. This suppression may eventually contribute to a well-known phenomenon called D1R-D2R synergy, which was demonstrated in numerous pharmacological studies and the studies using D1R or D2R knockout mice (reviewed in Holmes et al., 2004) and is needed for motor stimulation by psychostimulants.

Experimental Procedures

Animals

Adult male Wistar rats weighting 200–225 g (Charles River, New York, NY) were individually housed in clear plastic cages in a controlled environment at a constant temperature of 23°C and humidity of 50% ± 10% with food and water available ad libitum. The animal room was on a 12/12 hr light/dark cycle with lights on at 0700. Rats were allowed 6 days of habituation to the animal colony before any treatment began. All animal use procedures were in strict accordance with the NIH Guide for the Care and Use of Laboratory Animals and were approved by the Institutional Animal Care and Use Committee.

Cloning, Expression, and Purification of GST Fusion Proteins

The cDNA fragment encoding the D2R C-terminal region ($D2R_{CT}$, N430-C443), D2R second intracellular loop ($D2R_{IL2}$, S129-T153), D2R third intracellular loop ($D2R_{IL3}$, K211-Q373), $D2R_{IL3}$-1 (I210-V270), $D2R_{IL3}$-2 (G242-Q373), D3R second intracellular loop ($D3R_{IL2}$, S125-A151), D3R third intracellular loop ($D3R_{IL3}$, R210-K372), NMDAR NR1-1a subunit C-terminal region ($NR1\text{-}1a_{CT}$; E834-S938), or NMDAR NR2B subunit C-terminal region ($NR2B_{CT}$; E839-V1482) was generated by PCR amplification from full-length cDNA clones. These fragments were subcloned into BamHI-EcoRI sites of the pGEX4T-3 plasmid (Amersham Biosciences, Arlington Heights, IL) or SpeI-XhoI sites of the pET-41a(+) plasmid (Novagen, Madison, WI). Initiation methionine residues and stop codons were also incorporated where appropriate. To confirm appropriate splice fusion, all constructs were resequenced. GST fusion proteins were expressed in *E. coli* BL21 competent cells (Amersham) or BL21(DE3)pLysE competent cells (Novagen) and purified from bacterial lysates as described by the manufacturer.

Affinity Purification, or Pull-Down, Assay

The solubilized striatal extracts (50–100 μg of protein) were diluted with 1× PBS/1% Triton X-100 and incubated with 50% (v/v) slurry of glutathione-sepharose 4B beads (Amersham) saturated with the GST protein alone or indicated GST fusion proteins (15 μg) for 2–3 hr at 4°C. Beads were washed four times with 1× PBS/1% Triton X-100. Bound proteins were eluted with 2× LDS loading buffer and were resolved by SDS-PAGE and immunoblotted with respective antibodies.

Blot Overlay Assay

GST fusion proteins were fractionated by SDS-PAGE and transferred to a PVDF membrane. After blocking (5% milk in PBS and 0.1% Tween 20), the membrane was incubated in 2% milk-PBS buffer containing 2.5–5 μg/ml of a purified protein probe for 2 hr at room temperature. The bound protein was revealed by standard western blot analysis using a respective antibody.

In Vitro Binding Assay

GST-$NR2B_{CT}$ (5 μg) in PBS was digested with 0.2 NIH unit of thrombin (Sigma, St. Louis, MO) for 2 hr at room temperature. The reaction was stopped by adding PMSF (10 μM), and the mixture was incubated for 1 hr at 4°C. GST was removed by glutathione-sepharose (Amersham). The supernatant was equilibrated to a final 1× binding buffer (200 mM NACl, 0.2% Triton X-100, 0.2 mg/ml BSA, and 50 mM Tris [pH, 7.5]). Binding reaction was initiated by adding GST-$D2R_{IL3}$, GST-$D2R_{IL3\text{-}1}$, GST-$D2R_{IL3\text{-}2}$, or GST-$D3R_{IL3}$ and incubated for 2–3 hr at 4°C. GST fusion proteins were precipitated using 100 μl of 10% glutathione-sepharose. The precipitate was washed three times with 1× binding buffer. Bound proteins were eluted with 2× LDS loading buffer and were resolved by SDS-PAGE.

Coimmunoprecipitation

Protein samples (PSD or P2 fraction) from the striatum, the hippocampus, or the frontal cortex were used for coimmunoprecipitation (Mao et al., 2005). NR2B and D2R were precipitated using a respective rabbit polyclonal antibody against NR2B (Chemicon, Temecula, CA) and D2R (Chemicon) and 50% protein A agarose/sepharose bead slurry (Amersham). Proteins were separated on Novex 4%–12% gels and probed with a rabbit antibody against NR2B (Chemicon), D2R (Chemicon), D1R (Chemicon), phospho-CaMKIIα-Tyr^{286} (Santa Cruz Biotechnology, Santa Cruz, CA), or CaMKIIα (Santa Cruz). HRP-conjugated secondary antibodies and enhanced chemiluminescence were used to detect proteins.

Acute Isolation of Striatal Neurons and Electrophysiology

Rat striatal neurons were acutely isolated according to our previously described technique (Xiong et al., 1999). Briefly, Wistar rats (1–2 weeks) were anesthetized and sacrificed. The whole brain was removed and sectioned (400 μm). The slices were then digested with papain (0.3–0.5 mg/ml). For the isolation, the striatal region was cut out in a culture dish under a microscope. Single cells were mechanically dissociated using fire-polished glass pipettes. Electrophysiological recording began approximately 20 min after the mechanical dissociation.

Whole-cell patch-clamp recordings were performed as described previously (Xiong et al., 2004). The recordings were only made on medium-sized neurons, which were easy to distinguish from large-sized cells based on somatic cross-sectional size and membrane capacitance. Patch electrodes (2 to ∼3 MΩ) were constructed from thin-walled borosilicated glass. A multibarrel perfusion system was employed to achieve a rapid exchange of extracellular solutions. Whole-cell currents were recorded using Axopatch 1D or 200B amplifiers (Axon Instruments, Foster City, CA). Data were filtered at 2 kHz and digitized at 5 Hz using a Digidata 1320 DAC unit (Axon Instruments). The online acquisition was done using pCLAMP software (Version 8, Axon Instruments). Standard extracellular solutions contained 140 mM NaCl, 5.4 mM KCl, 2.0 mM $CaCl_2$, 20 mM HEPES, and 10 mM glucose (pH 7.4; 320 to ∼330 mOsm). The pipette solution contained 140 mM CsF, 10 mM HEPES, 11 mM EGTA, 2 mM TEA, 1 mM $CaCl_2$, 2 mM $MgCl_2$, and 4 mM K_2ATP (pH 7.3; 300 mOsm). In general, NMDAR currents were activated by applying NMDA (100 μM) together with glycine (3 μM) every 1 min to allow for a complete recovery of the channels from desensitization. During each experiment, a voltage step of −10 mV from the holding potential was applied periodically to monitor cell capacitance and access resistance. Recordings in which access resistance or capacitance changed by more than 10% during the experiment were not included in data analysis.

Behavioral Assessments

Locomotion in an open field was evaluated with an infrared photocell-based, automated Opto-Varimex-Micro apparatus (Columbus Instruments, Columbus, OH) under illuminated conditions in a sound-attenuated room. Rats were placed in an activity chamber and were habituated to the chamber environment for 2 hr. Three sensor pairs positioned in x, y (horizontal), and z (vertical, above the animal's normal height) directions were assigned to each animal cage to provide information about horizontal and vertical activities, which were recorded at 5 min intervals before and after drug injection. Each sensor pair produces 16 infrared light beams intersecting the animal cage (beam scan rate = 10 Hz). Status about infrared beam interruptions by presence of animals was transferred from all sensors to a computer with operating software. Stereotypy was detected using computer-generated stereotypy time recorded by Opto-Varimex-Micro monitors, which refers to the total time that stereotypic behaviors (repetitive breaks of a given beam or beams with an interval less than 1 s) were observed.

Supplemental Data

The Supplemental Data for this article can be found online at http://www.neuron.org/cgi/content/full/52/5/897/DC1/.

Acknowledgments

This work was supported by the NIH grants DA010355 (J.Q.W.) and MH061469 (J.Q.W.). We thank Dr. Xiaoqiang Yu, Dr. Nilofer Qureshi, and Brian Vukusic for technical support and comments, and Dr. Yves Auberson for providing NVP-AAM077.

Received: April 21, 2006
Revised: September 2, 2006
Accepted: October 5, 2006
Published: December 6, 2006

References

Aizman, O., Brismar, H., Uhlen, P., Zettergren, E., Levey, A.I., Forssberg, H., Greengard, P., and Aperia, A. (2000). Anatomical and physiological evidence for D1 and D2 dopamine receptor colocalization in neostriatal neurons. Nat. Neurosci. *3*, 226–230.

Auberson, Y.P., Allgeier, H., Bischoff, S., Lingenhoehl, K., Moretti, R., and Schmutz, M. (2002). 5-Phosphonomethylquinoxalinediones as competitive NMDA receptor antagonists with a preference for the human 1A/2A, rather than 1A/2B receptor composition. Bioorg. Med. Chem. Lett. *12*, 1099–1102.

Berke, J.D., and Hyman, S.E. (2000). Addiction, dopamine, and the molecular mechanisms of memory. Neuron *25*, 515–532.

Bibb, J.A. (2005). Decoding dopamine signaling. Cell *122*, 153–155.

Bofill-Cardona, E., Kudlacek, O., Yang, Q., Ahorn, H., Freissmuth, M., and Nanoff, C. (2000). Binding of calmodulin to the D_2-dopamine receptor reduces receptor signaling by arresting the G protein activation switch. J. Biol. Chem. *275*, 32672–32680.

Boudreau, A.C., and Wolf, M.E. (2005). Behavioral sensitization to cocaine is associated with increased AMPA receptor surface expression in the nucleus accumbens. J. Neurosci. *25*, 9144–9151.

Chang, B.H., Mukherji, S., and Soderling, T.R. (1998). Characterization of a calmodulin kinase II inhibitor protein in brain. Proc. Natl. Acad. Sci. USA *95*, 10890–10895.

Chen, Q., and Reiner, A. (1996). Cellular distribution of the NMDA receptor NR2A/2B subunits in the rat striatum. Brain Res. *743*, 346–352.

Chung, H.J., Huang, Y.H., Lau, L.F., and Huganir, R.L. (2004). Regulation of the NMDA receptor complex and trafficking by activity-dependent phosphorylation of the NR2B subunit PDZ ligand. J. Neurosci. *24*, 10248–10259.

Dunah, A.W., Sirianni, A.C., Fienberg, A.A., Bastia, E., Schwarzschild, M.A., and Standaert, D.G. (2004). Dopamine D1-dependent trafficking of striatal N-methyl-D-aspartate glutamate receptors requires Fyn protein tyrosine kinase but not DARPP-32. Mol. Pharmacol. *65*, 121–129.

Fiorentini, C., Gardoni, F., Spano, P., Di Luca, M., and Missale, C. (2003). Regulation of dopamine D_1 receptor trafficking and desensitization by oligomerization with glutamate *N*-methyl-D-aspartate receptors. J. Biol. Chem. *278*, 20196–20202.

Fischer, G., Mutel, V., Trube, G., Malherbe, P., Kew, J.N., Mohacsi, E., Heitz, M.P., and Kemp, J.A. (1997). Ro 25-6981, a highly potent and selective blocker of *N*-methyl-D-aspartate receptors containing the NR2B subunit. Characterization *in vitro*. J. Pharmacol. Exp. Ther. *283*, 1285–1292.

Flores-Hernandez, J., Cepeda, C., Hernandez-Echeagaray, E., Calvert, C.R., Jokel, E.S., Fienberg, A.A., Greengard, P., and Levine, M.S. (2002). Dopamine enhancement of NMDA currents in dissociated medium-sized striatal neurons: role of D1 receptors and DARPP-32. J. Neurophysiol. *88*, 3010–3020.

Gardoni, F., Caputi, A., Cimino, M., Pastorino, L., Cattabeni, F., and Di Luca, M. (1998). Calcium/calmodulin-dependent protein kinase II is associated with NR2A/B subunits of NMDA receptor in postsynaptic densities. J. Neurochem. *71*, 1733–1741.

Gerfen, C.R. (2000). Molecular effects of dopamine on striatal-projection pathways. Trends Neurosci. *23*, S64–S70.

Graybiel, A.M., Ragsdale, C.W., Jr., Yoneoka, E.S., and Elde, R.P. (1981). An immunohistochemical study of enkephalins and other neuropeptides in the striatum of the cat with evidence that the opiate peptides are arranged to form mosaic patterns in register with the striosomal compartments visible by acetylcholinersterase staining. Neuroscience *6*, 377–397.

Hall, R.A., and Soderling, T.R. (1997). Differential surface expression and phosphorylation of the *N*-methyl-D-aspartate receptor subunits NR1 and NR2 in cultured hippocampal neurons. J. Biol. Chem. *272*, 4135–4140.

Hersch, S.M., Ciliax, B.J., Gutekunst, C.A., Rees, H.D., Heilman, C.J., Yung, K.K.L., Bolam, J.P., Ince, E., Yi, H., and Levey, A.I. (1995). Electron microscopic analysis of D1 and D2 dopamine receptor proteins in the dorsal striatum and their synaptic relationships with motor corticostriatal afferents. J. Neurosci. *15*, 5222–5237.

Holmes, A., Lachowicz, J.E., and Sibley, D.R. (2004). Phenotypic analysis of dopamine receptor knockout mice; recent insights into the functional specificity of dopamine receptor subtypes. Neuropharmacology *47*, 1117–1134.

Hurd, Y.L., and Ungerstedt, U. (1989). Cocaine: an *in vivo* microdialysis evaluation of its acute action on dopamine transmission in rat striatum. Synapse *3*, 48–54.

Hyman, S.E., and Malenka, R.C. (2001). Addiction and the brain: the neurobiology of compulsion and its persistence. Nat. Rev. Neurosci. *2*, 695–703.

Kalivas, P.W. (2004). Glutamate systems in cocaine addiction. Curr. Opin. Pharmacol. *4*, 23–29.

Kalivas, P.W., and Duffy, P. (1993). Time course of extracellular dopamine and behavioral sensitization to cocaine. I. Dopamine axon terminals. J. Neurosci. *13*, 266–275.

Kelly, P.T., McGuinness, T.L., and Greengard, P. (1984). Evidence that the major postsynaptic density protein is a component of a Ca^{2+}/calmodulin-dependent protein kinase. Proc. Natl. Acad. Sci. USA *81*, 945–949.

Koob, G.F., and Nestler, E.J. (1997). The neurobiology of drug addiction. J. Neuropsychiatry Clin. Neurosci. *9*, 482–497.

Kotecha, S.A., Oak, J.N., Jackson, M.F., Perez, Y., Orser, B.A., Van Tol, H.H.M., and MacDonald, J.F. (2002). A D2 class dopamine receptor transactivates a receptor tyrosine kinase to inhibit NMDA receptor transmission. Neuron *35*, 1111–1122.

Kuppenbender, K.D., Standaert, D.G., Feuerstein, T.J., Penney, J.B., Jr., Young, A.B., and Landwehrmeyer, G.B. (2000). Expression of NMDA receptor subunit mRNAs in neurochemically identified projection neurons and interneurons in the human striatum. J. Comp. Neurol. *419*, 407–421.

Landwehrmeyer, G.B., Standaert, D.G., Testa, C.M., Penney, J.B., Jr., and Young, A.B. (1995). NMDA receptor subunit mRNA expression by projection neurons and interneurons in rat striatum. J. Neurosci. *15*, 5297–5307.

Lau, L.F., and Huganir, R.L. (1995). Differential tyrosine phosphorylation of *N*-methyl-D-aspartate receptor subunits. J. Biol. Chem. *270*, 20036–20041.

Lee, F.J.S., Xue, S., Pei, L., Vukusic, B., Chery, N., Wang, Y., Wang, Y.T., Niznik, H.B., Yu, X.M., and Liu, F. (2002). Dual regulation of NMDA receptor functions by direct protein-protein interactions with the dopamine D1 receptor. Cell *111*, 219–230.

Liao, G.Y., Wagner, D.A., Hsu, M.H., and Leonard, J.P. (2001). Evidence for direct protein kinase-C mediated modulation of *N*-methyl-D-aspartate receptor current. Mol. Pharmacol. *59*, 960–964.

Lieberman, D.N., and Mody, I. (1994). Regulation of NMDA channel function by endogenous Ca(2+)-dependent phosphatase. Nature *369*, 235–239.

Lindgren, N., Usiello, A., Goiny, M., Haycock, J., Erbs, E., Greengard, P., Hokfelt, T., Borrelli, E., and Fisone, G. (2003). Distinct roles of dopamine D2L and D2S receptor isoforms in the regulation of protein phosphorylation at presynaptic and postsynaptic sites. Proc. Natl. Acad. Sci. USA *100*, 4305–4309.

Mao, L., Yang, L., Tang, Q., Samdani, S., Zhang, G., and Wang, J.Q. (2005). The scaffold protein homer1b/c links metabotropic glutamate receptor 5 to extracellular signal-regulated protein kinase cascades in neurons. J. Neurosci. *25*, 2741–2752.

Nakazawa, T., Komai, S., Tezuka, T., Hisatsune, C., Umemori, H., Semba, K., Mishina, M., Manabe, T., and Yamamoto, T. (2001). Characterization of Fyn-mediated tyrosine phosphorylation sites on GluR epsilon 2 (NR2B) subunit of the N-methyl-D-aspartate receptor. J. Biol. Chem. *276*, 693–699.

Nestler, E.J. (2005). Is there a common molecular pathway for addiction. Nat. Neurosci. *8*, 1445–1449.

Neyton, J., and Paoletti, P. (2006). Relating NMDA receptor function to receptor subunit composition: limitations of the pharmacological approach. J. Neurosci. *26*, 1331–1333.

Omkumar, R.V., Melinda, O., Kiely, M.J., Rosenstein, A.J., Min, K.T., and Kennedy, M.B. (1996). Identification of a phosphorylation site for calcium/calmodulin-dependent protein kinase II in the NR2B subunit of the *N*-methyl-D-aspartate receptor. J. Biol. Chem. *271*, 31670–31678.

Rostas, J.A., Brent, V.A., Voss, K., Errington, M.L., Bliss, T.V., and Gurd, J.W. (1996). Enhanced tyrosine phosphorylation of the 2B subunit of the *N*-methyl-D-aspartate receptor in long-term potentiation. Proc. Natl. Acad. Sci. USA *93*, 10452–10456.

Sattler, R., and Tymianski, M. (2001). Molecular mechanisms of glutamate receptor-mediated excitotoxic neuronal cell death. Mol. Neurobiol. *24*, 107–129.

Sesack, S.R., Carr, D.B., Omelchenko, N., and Pinto, A. (2004). Anatomical substrates for glutamate-dopamine interactions: evidence for specificity of connections and extrasynaptic actions. In Glutamate and Disorders of Cognition and Motivation, *Volume 1003*, B. Moghaddam and M.E. Wolf, eds. (New York: New York Academy of Sciences), pp. 36–52.

Sheng, M., and Kim, M.J. (2002). Postsynaptic signaling and plasticity mechanisms. Science *298*, 776–780.

Soderling, T.R. (2000). CaM-kinases: modulators of synaptic plasticity. Curr. Opin. Neurobiol. *10*, 375–380.

Standaert, D.G., Friberg, I.K., Landwehrmeyer, G.B., Young, A.B., and Penney, J.B., Jr. (1999). Expression of NMDA glutamate receptor subunit mRNAs in neurochemically identified projection and interneurons in the striatum of the rat. Brain Res. Mol. Brain Res. *64*, 11–23.

Surmeier, D.J., Song, W.J., and Yan, Z. (1996). Coordinated expression of dopamine receptors in neostriatal medium spiny neurons. J. Neurosci. *16*, 6579–6591.

Svenningsson, P., Nairn, A.C., and Greengard, P. (2005). DARPP-32 mediates the actions of multiple drugs of abuse. AAPS J. *7*, E353–E360.

Szumlinski, K.K., Dehoff, M.H., Kang, S.H., Frys, K.A., Lominac, K.D., Klugmann, M., Rohrer, J., Griffin, W., 3rd, Toda, S., Champtiaux, N.P., et al. (2004). Homer proteins regulate sensitivity to cocaine. Neuron *43*, 401–413.

Tingley, W.G., Ehlers, M.D., Kameyama, K., Doherty, C., Ptak, J.B., Riley, C.T., and Huganir, R.L. (1997). Characterization of protein kinase A and protein kinase C phosphorylation of the *N*-methyl-D-aspartate receptor NR1 subunit using phosphorylation site-specific antibodies. J. Biol. Chem. *272*, 5157–5166.

Usiello, A., Baik, J.H., Rouge-Pont, F., Picetti, R., Dierich, A., LeMeur, M., Piazza, P.V., and Borreli, E. (2000). Distinct functions of the two isoforms of dopamine D2 receptors. Nature *408*, 199–203.

Valjent, E., Corvol, J.C., Pages, C., Besson, M.J., Maldonado, R., and Caboche, J. (2000). Involvement of the extracellular signal-regulated kinase cascade for cocaine-rewarding properties. J. Neurosci. *20*, 8701–8709.

Vanderschuren, L.J., and Kalivas, P.W. (2000). Alterations in dopaminergic and glutamatergic transmission in the induction and expression of behavioral sensitization: a critical review of preclinical studies. Psychopharmacology (Berl.) *151*, 99–120.

Wang, H., and Pickel, V.M. (2002). Dopamine D2 receptors are present in prefrontal cortical afferents and their targets in patches of the rat caudate-putamen nucleus. J. Comp. Neurol. *442*, 392–404.

Wang, J.Q., and McGinty, J.F. (1999). Glutamate/dopamine interactions mediate the effects of psychostimulant drugs. Addict. Biol. *4*, 141–150.

Wang, L.Y., Taverna, F.A., Huang, X.P., MacDonald, J.F., and Hampson, D.R. (1993). Phosphorylation and modulation of a kainate receptor (GluR6) by cAMP-dependent protein kinase. Science *259*, 1173–1175.

Wang, Y.T., and Salter, M.W. (1994). Regulation of NMDA receptors by tyrosine kinases and phosphatases. Nature *369*, 233–235.

Wolf, M.E. (1998). The role of excitatory amino acids in behavioral sensitization to psychomotor stimulants. Prog. Neurobiol. *54*, 679–720.

Xiong, Z.G., Pelkey, K.A., Lu, W.Y., Lu, Y.M., Roder, J.C., MacDonald, J.F., and Salter, M.W. (1999). Src potentiation of NMDA receptors in hippocampal and spinal neurons is not mediated by reducing zinc inhibition. J. Neurosci. *19*, RC37.

Xiong, Z.G., Zhu, X.M., Chu, X.P., Minami, M., Hey, J., Wei, W.L., MacDonald, J.F., Wemmie, J.A., Price, M.P., Welsh, M.J., and Simon, R.P. (2004). Neuroprotection in ischemia: blocking calcium-permeable Acid-sensing ion channels. Cell *118*, 687–698.

Yao, W.D., Gainetdinov, R.R., Arbuchle, M.I., Sotnikova, T.D., Cyr, M., Beaulieu, J.M., Torres, G.E., Grant, S.G., and Caron, M.G. (2004). Identification of PSD-95 as a regulator of dopamine-mediated synaptic and behavioral plasticity. Neuron *41*, 625–638.

Yung, K.K., and Bolam, J.P. (2000). Localization of dopamine D1 and D2 receptors in the rat neostriatum: synaptic interaction with glutamate- and GABA-containing axonal terminals. Synapse *38*, 413–420.

Zhang, L., Lou, D., Jiao, H., Zhang, D., Wang, X., Xia, Y., Zhang, J., and Xu, M. (2004). Cocaine-induced intracellular signaling and gene expression are oppositely regulated by the dopamine D1 and D3 receptors. J. Neurosci. *24*, 3344–3354.

Zorumski, C.F., and Izumi, Y. (1998). Modulation of LTP induction by NMDA receptor activation and nitric oxide release. Prog. Brain Res. *118*, 173–182.